Bioorganic & Medicinal Chemistry Letters 18 (2008) 6352–6356

Contents lists available at ScienceDirect

Bioorganic & Medicinal Chemistry Letters

journal homepage: www.elsevier.com/locate/bmcl

Identification and optimization of N^3,N^6-diaryl-1*H*-pyrazolo[3,4-*d*] pyrimidine-3,6-diamines as a novel class of ACK1 inhibitors

David J. Kopecky [a,*], Xiaolin Hao [a], Yi Chen [a], Jiasheng Fu [a], XianYun Jiao [a], Juan C. Jaen [e], Mario G. Cardozo [b], Jinsong Liu [b], Zhulun Wang [b], Nigel P. C. Walker [b], Holger Wesche [c], Shyun Li [c], Ellyn Farrelly [d], Shou-Hua Xiao [d], Frank Kayser [a,*]

[a] Department of Chemistry, Amgen Inc., 1120 Veterans Boulevard, South San Francisco, CA 94080, USA
[b] Department of Molecular Structure, Amgen Inc., 1120 Veterans Boulevard, South San Francisco, CA 94080, USA
[c] Department of Oncology, Amgen Inc., 1120 Veterans Boulevard, South San Francisco, CA 94080, USA
[d] Department of Lead Discovery, Amgen Inc., 1120 Veterans Boulevard, South San Francisco, CA 94080, USA
[e] ChemoCentryx Inc., 850 Maude Avenue, Mountain View, CA 94043, USA

ARTICLE INFO

Article history:
Received 30 August 2008
Revised 16 October 2008
Accepted 20 October 2008
Available online 1 November 2008

Keywords:
ACK1
Kinase inhibitor
Cancer
SAR
Pyrazolo[3,4,-*d*]pyrimidine-3,6-diamine

ABSTRACT

A new series of pyrazolo[3,4-*d*]pyrimidine-3,6-diamines was designed and synthesized as potent and selective inhibitors of the nonreceptor tyrosine kinase, ACK1. These compounds arose from efforts to rigidify an earlier series of *N*-aryl pyrimidine-5-carboxamides. The synthesis and structure–activity relationships of this new series of inhibitors are reported. The most promising compounds were also profiled for their pharmacokinetic properties.

ACK1 (Activated Cdc42Hs-associated Kinase 1) is a nonreceptor tyrosine kinase that was first identified by its interaction with Cdc42 and was suggested to function as an effector of Cdc42, Rac, and FAK in several integrin signaling pathways.[1] ACK1 has also been identified as a regulator of endocytosis via direct association with clathrin.[2] ACK1 is ubiquitously expressed, with highest expression levels in the brain, and has been shown to be overexpressed in a number of human tumor cell lines potentially predisposing them to become metastatic.[3] Recently it was suggested that ACK1 activity is required for the survival of v-RAS-transformed murine fibroblasts.[3] Moreover, activation of ACK1 has been shown to stimulate prostate tumorigenesis.[4] These findings suggest that inhibition of ACK1 could be a potential new point of intervention in preventing the onset and spread of cancer. The development of a potent and selective ACK1 inhibitor would allow the role of ACK1 in tumor progression to be probed. Toward this end, herein we report on a new class of ACK1 inhibitors.

During the course of our ACK1 inhibitor program, a high-throughput screening (HTS) campaign of our internal sample collection was conducted. A series of *N*-aryl pyrimidine-5-carboxam-

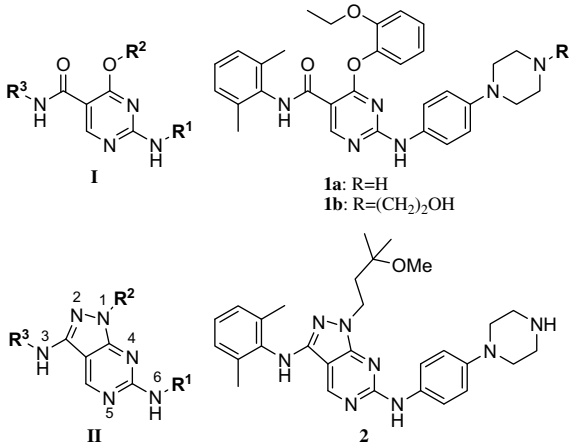

Figure 1. N^3,N^6-diaryl-1*H*-pyrazolo[3,4-*d*]pyrimidine-3,6-diamine lead structure **II** where $\mathbf{R^2}$ is a functionalized aliphatic chain. Nitrogen atom numbering is shown.

* Corresponding authors. Tel.: +1 650 244 2146; fax: +1 650 837 9369 (D.J.Kopecky); tel.: +1 650 244 2062 (F.Kayser).
E-mail addresses: dkopecky@amgen.com (D.J. Kopecky), fkayser@amgen.com (F. Kayser).

0960-894X/$ - see front matter © 2008 Elsevier Ltd. All rights reserved.
doi:10.1016/j.bmcl.2008.10.092

ides of the general structure **I** (Fig. 1) was identified. Earlier studies of the structure–activity relationship (SAR) of **I** identified compound **1a** as one of the more potent inhibitors within this series in both biochemical and cellular autophosphorylation assays.[5–7] (ACK1 K_i = 0.02 μM, Cell IC_{50} = 0.1 μM). Unfortunately, this compound series generally displayed poor selectivity against several other kinases (data not shown) and a poor pharmacokinetic profile in male Sprague–Dawley rats (**1a**: Cl = 3.8 L/h/kg, AUC = 76 μg h/L; 0.4 mg/kg iv).

The X-ray co-crystal structure of the close analog **1b** bound to the ACK1 catalytic kinase domain was subsequently determined at 2.3 Å resolution (Fig. 2). Inspection of the three-dimensional structure of the complex revealed a binding mode in which the aminopyrimidine moiety participates in key hinge interactions: the pyrimidine nitrogen forms a hydrogen bond with the NH from Ala208, and the carbonyl of Ala208 H-bonds to the NH of the 2-amino group. The 4-position of the aryloxy moiety is oriented towards a solvent-exposed area, while the dimethyl-phenyl group is perfectly positioned to enter a deep hydrophobic pocket. Hydrophobic interactions within this selectivity pocket, combined with an additional H-bond with the conserved threonine (Thr205) gatekeeper amino-acid residue, are key features found in several potent kinase inhibitors, such as those described for the related tyrosine kinase p56^{lck} (LCK).[8]

Molecular modeling suggested that the inhibitory activity of series **I** might be improved upon by taking advantage of the additional Thr205 hydrogen bond. Following this rationale, several modifications of **I** were designed which tied the amide carbonyl and the ether oxygen into a cyclic structure, while rotating the NH into a more optimal position to interact with Thr205. The new designs were modeled into the ATP-binding site and the most promising candidates were selected for synthesis. These efforts identified N^3,N^6-diaryl-1*H*-pyrazolo[3,4-*d*]pyrimidine-3,6-diamines **II** as a novel series of inhibitors of ACK1, of which compound **2** is a representative example (Figs. 1 and 2).[9]

Compounds of the general structure **II** were synthesized as outlined in Scheme 1 by a five-step procedure. Chlorination of **3** was achieved with a mixture of PCl_5 and $POCl_3$. The resulting acid chloride was coupled with an appropriately substituted aniline in the presence of an acid-scavenger and then treated with 3-methyl-3-methoxybutylhydrazine[10] to produce **4**. Cyclization of **4** with PCl_5 in refluxing toluene gave **5**, and subsequent chloride displacement with an appropriate aniline provided compounds **2** and **6–19**. Early exploratory work on the new series established that a functionalized aliphatic chain at N-1 of the N^3,N^6-diaryl-1*H*-pyrazolo[3,4-*d*]pyrimidine-3,6-diamine core was beneficial for ACK1 inhibition. Also, the replacement of the aromatic groups at either N-3 or N-6 of the 1*H*-pyrazolo[3,4-*d*]pyrimidine-3,6-diamine scaffold with an alkyl group or a hydrogen led to significantly reduced levels of ACK1 inhibition (data not shown).

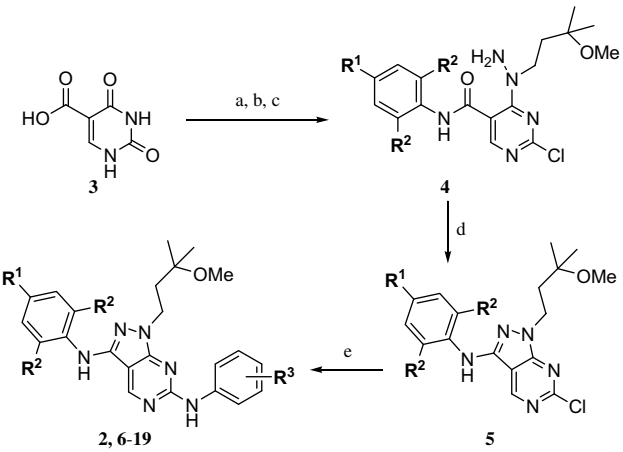

Scheme 1. Reagents and conditions: (a) PCl_5, $POCl_3$, reflux, quantitative; (b) Amberlyst A-21 resin, 2,6-di(**R²**)-4-(**R¹**)-aniline, EtOAc, 50 °C, 90%; (c) $(Me)_2(MeO)CCH_2CH_2NHNH_2$, Et_3N, THF, 75–85%; (d) PCl_5, toluene, reflux, 65–80%; (e) TFA, (**R³**)-aniline, 1,4-dioxane/*n*-BuOH, reflux, 50–70%.

Compound **2**, which possesses a 3-methyl-3-methoxybutyl substituent at N-1 (Table 1) showed significantly improved ACK1 inhibition over **1a** in both biochemical and cellular autophosphorylation assays.[6,7] Subsequent derivatives **6–19** demonstrated that both methyl and chloro were well tolerated at **R²** although hydrogen was not. Installation of larger groups at **R¹** such as methyl (compounds **10** and **19**) diminishes binding, presumably due to steric crowding at the rear of the small hydrophobic pocket that the N-3-substituent occupies. The effects of incorporating a smaller fluorine atom at **R¹** are less pronounced (compounds **9** and **18**).

The 4-position of the N-6-phenyl ring points out of the enzyme towards solvent, providing an area to introduce polar solubilizing groups for better cell penetration. As seen in Table 1, a variety of N- and O-linked groups were tolerated in this position without dramatically affecting enzyme inhibition. A 3-fluoro atom could also be introduced next to O-linked groups without affecting potency (compounds **14–16**). The 3-fluoro was introduced in an attempt to impart metabolic stability to the scaffold by stabilizing one of the two electron-rich aniline moieties present in the molecule. Furthermore, in the case of **15**, the other aniline moiety is simultaneously stabilized by 2,6-dichloro substitution.

Despite these efforts to prevent oxidative metabolic degradation, **15** and **16** showed only marginal improvements in metabolic stability and still exhibited high plasma clearances as shown in Table 2. High molecular weight as well as relative high *c*log *P* values could be contributing factors to the poor PK profiles of **15** and related derivatives.[11] We were pleased to discover several compounds with reduced molecular weight where **R³** is hydrogen which retain high levels of biochemical and cellular potency (Table 1, compounds **7** and **8**). At this stage, a thorough investigation of the N-1 substituent was desired prior to readdressing the issue of metabolic stability for these truncated analogs.

A high-resolution X-ray co-crystal structure of **2** complexed to ACK1 was obtained (Fig. 3). As predicted in our earlier modeling, two hydrogen bonds to the hinge region of the ACK1 ATP-binding site along with an additional H-bond to the carbonyl oxygen of

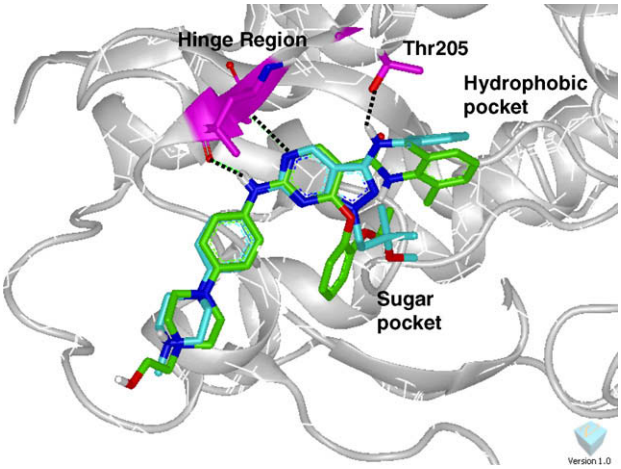

Figure 2. Overlap of high-resolution X-ray co-crystal structure of original hit **1b** (green) bound to ACK1, and the binding mode model for compound **2** (cyan). RCSB file name (3EQP).

Table 1
ACK1 inhibition for N^3,N^6-diaryl-N^1-(3,3-dimethyl-3-methoxypropyl)pyrazolopyrimidine-3,6-diamines **2** and **6–19**

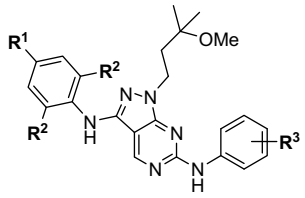

Compound	R^1	R^2	R^3	ACK1 K_i[a] (μM)	ACK1 cell IC_{50}[b] (μM)
2	H	Me	4-Piperazin-1-yl	0.002	0.01
6	H	H	H	>4	ND
7	H	Me	H	0.003	0.02
8	H	Cl	H	0.007	0.04
9	F	Me	H	0.026	5.5
10	Me	Me	H	>2.5	ND
11	H	Cl	4-Piperazin-1-yl	0.012	0.01
12	H	Me	4-(4-Methylpiperazin-1-yl)	0.002	0.02
13	H	Me	4-$O(CH_2)_2N(CH_2)_4$	0.003	0.02
14	H	Me	3-F, 4-$O(CH_2)_2N(CH_2)_4$	0.003	0.02
15	H	Cl	3-F, 4-$O(CH_2)_2N(CH_2)_4$	0.002	0.03
16	H	Me	3-F, 4-$O(CH_2)_3N(CH_2)_5$	0.003	0.06
17	H	H	4-(4-Methylpiperazin-1-yl)	0.4	2.1
18	F	Me	4-(4-Methylpiperazin-1-yl)	0.018	0.02
19	Me	Me	4-(4-Methylpiperazin-1-yl)	0.012	0.05

[a] Values are means of at least two experiments.
[b] Average of at least two IC_{50} values. ND, not determined.

Thr205 serve to anchor **2** into the binding pocket. In addition, the dimethyl-phenyl group makes a deeper contact in the hydrophobic selectivity pocket as compared to the amide series **I**. Moreover, two regions of **2** are exposed to solvent. The polar piperazine moiety directly faces the solvent, creating a stabilizing interaction that aids in inhibitor binding or recognition. Also, the terminus of the N-1 side chain is exposed to solvent by protruding through a lipophilic channel present in the phosphate-binding region of the active site. The latter observation served to guide subsequent SAR work: It was hoped that binding could be improved by strengthening the solubilizing interaction between the terminus of the N-1 side chain and exposed solvent while maintaining a low overall molecular weight by keeping the N-6 phenyl ring unsubstituted.

Table 2
Pharmacokinetic parameters following iv dose in male Sprague–Dawley rats.[a,b]

Compound	CL (L/h/kg)	V_{ss} (L/kg)	MRT (h)	AUC (μgh/L)
2	5.7	20.3	3.5	104
11	4.2	15.4	3.6	117
15	2.9	7.7	2.7	174
16	3.5	7.5	2	148

[a] $n = 3$ animals per study.
[b] Dosed at 0.5 mg/kg iv.

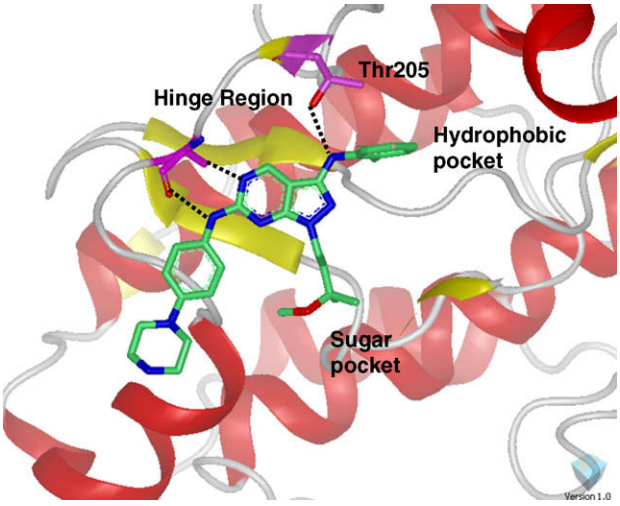

Figure 3. Actual high-resolution X-ray co-crystal structure of compound **2** bound to the ACK1 kinase domain. RCSB file name (3EQR).

A variety of N^3-(aryl)-N^6-(phenyl)-1*H*-pyrazolo[3,4-*d*]pyrimidine-3,6-diamines possessing polar solubilizing groups linked to N-1 by a one- to three-carbon spacer were synthesized and tested (Table 3). While most of the cyclic amine derivatives **20**–**24** (two-carbon spacer) were potent inhibitors of ACK1, inhibition was weakened when an amide linker was employed (compounds **25** and **26**). Non-cyclic amino groups attached to two- and three-carbon linkers were also investigated. While the *N*,*N*-dimethylaminoethyl derivative **27** exhibited slightly reduced cellular potency, the *N*,*N*-dimethylaminopropyl derivatives **28** and **29** strongly inhibited ACK1 (K_i of 5 nM and cellular IC_{50} of 20 nM for **28**). Replacing the dimethylamine with the more lipophilic diethylamine and pyrrolidine groups (compounds **30** and **31**) led to reduced cellular activities compared to **29**. Oxygenated carbon chains at R^2 were also investigated (Table 2, compounds **32**–**34**). The diols **32** and **33** exhibited excellent biochemical and cellular potencies that were comparable to those of **28** and **29**. However, ACK1 inhibition was weakened in converting the primary alcohol of **33** into a dimethylamine (compound **34**).

Compounds **20–24, 27**, and **36–38** were each synthesized by a five-step process from **3** and an appropriately mono-substituted hydrazine[10] as described above (Scheme 2). Compound **36** was further transformed into either **25** or **26** by ester hydrolysis followed by BOPCl-mediated amide formation (Scheme 3). The synthesis of derivatives **28**-**34** is detailed in Scheme 4. Dihydroxylation of either **37** or **38** with a mixture of OsO_4 and NMO generated **32** and **33**, respectively. Reductive amination of the aldehyde derived from diol **32** or **33** produced **28**–**31**, respectively. Compound **33** was transformed into **39** by selective tosylation of the primary

Table 3
ACK1 inhibition for N^3-(aryl)-N^6-(phenyl) pyrazolopyrimidine-3,6-diamines with selected *N*-1 substituents **R**^{1}.

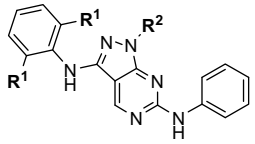

Compound	**R**^{1}	R^2	ACK1 K_i[a] (μM)	ACK1 cell IC_{50}[b] (μM)
7	Me	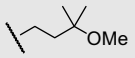	0.003	0.02
8	Cl	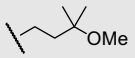	0.007	0.04
20	Cl	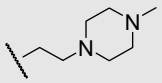	0.01	0.03
21	Cl	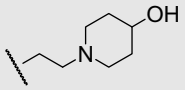	0.05	0.03
22	Me	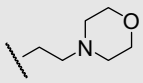	0.05	0.07
23	Cl	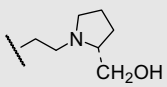	0.03	0.05
24	Cl	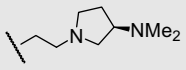	0.01	0.02
25	Cl		0.03	0.09
26	Cl	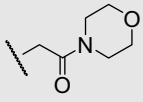	0.07	0.14
27	Cl	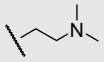	0.005	0.14
28	Cl	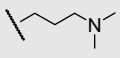	0.005	0.02
29	Me	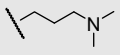	0.03	0.04
30	Me	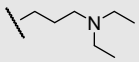	0.04	0.14
31	Me	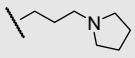	0.1	0.3
32	Cl	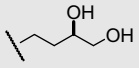	0.01	0.02
33	Me	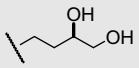	0.03	0.06
34	Me	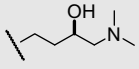	0.08	0.19

[a] Values are means of at least two experiments.
[b] Average of at least two IC_{50} values.

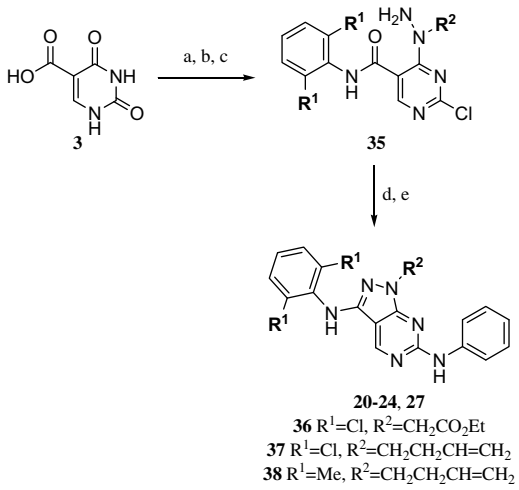

Scheme 2. Reagents and conditions: (a) PCl_5, $POCl_3$, reflux, quantitative; (b) Amberlyst A-21 resin, 2,6-di(**R**^{1})-aniline, EtOAc, 50 °C, 90%; (c) **R**^{2}$NHNH_2$, Et_3N, THF, 55–85%; (d) PCl_5, toluene, reflux, 50–80%; (e) TFA, aniline, 1,4-dioxane/*n*-BuOH or 1,4-dioxane, reflux, 55–90%.

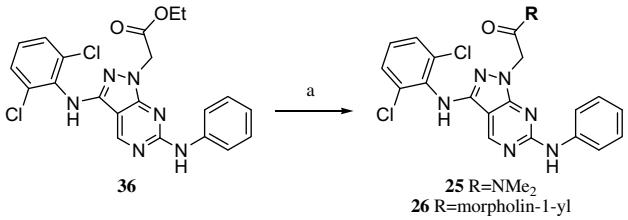

Scheme 3. Reagents: (a) i—aq KOH, MeOH; ii—BOPCl, **R**H, Et_3N, CH_2Cl_2, 90%.

alcohol followed by epoxide formation with NaOMe. Finally, **34** was obtained from **39** in low yield by exposure to dimethylamine in ethanol.

The biological data in Table 3 show that structural manipulation did not significantly affect ACK1 inhibitory activity (Table 1). However, a moderate improvement in PK properties was observed for a key analog. The male Sprague–Dawley rat pharmacokinetic profile of **32**, one of the most potent analogs in Table 3, showed a significant improvement in oral bioavailability relative to earlier analogs (F = 30%; 4 mg/kg po dose).

Modulation of selectivity for ACK1 over other related kinases was possible for this series by way of small structural changes. As an example, compound **13** displayed good selectivity against the related kinases KDR, Tie-2, and Jak3, but very potently inhibits BTK and LCK, which possess high structural similarity to ACK1 (Table 4). However, modification of the structure of **13** to include a single fluorine atom on the N-6 phenyl ring (compound **14**) eliminated binding to KDR, Tie-2, and Jak3, while greatly diminishing binding to both LCK and BTK relative to ACK1.

In conclusion, we have demonstrated that N^3,N^6-diaryl-1*H*-pyrazolo[3,4-*d*]pyrimidine-3,6-diamines represent a novel class of ACK1 inhibitors. The presence of a polar substituent at C-4 of the N-6 aryl ring was shown to be unnecessary for maintaining high levels of inhibitory activity. Furthermore, selectivity for ACK1 over some related kinases could be achieved via minimal structural modifications. Despite non-optimal pharmacokinetic profiles, these highly potent analogs represent a promising new lead series of ACK1 inhibitors which, with further study, may prove useful for identifying compounds suitable for in vivo experiments.

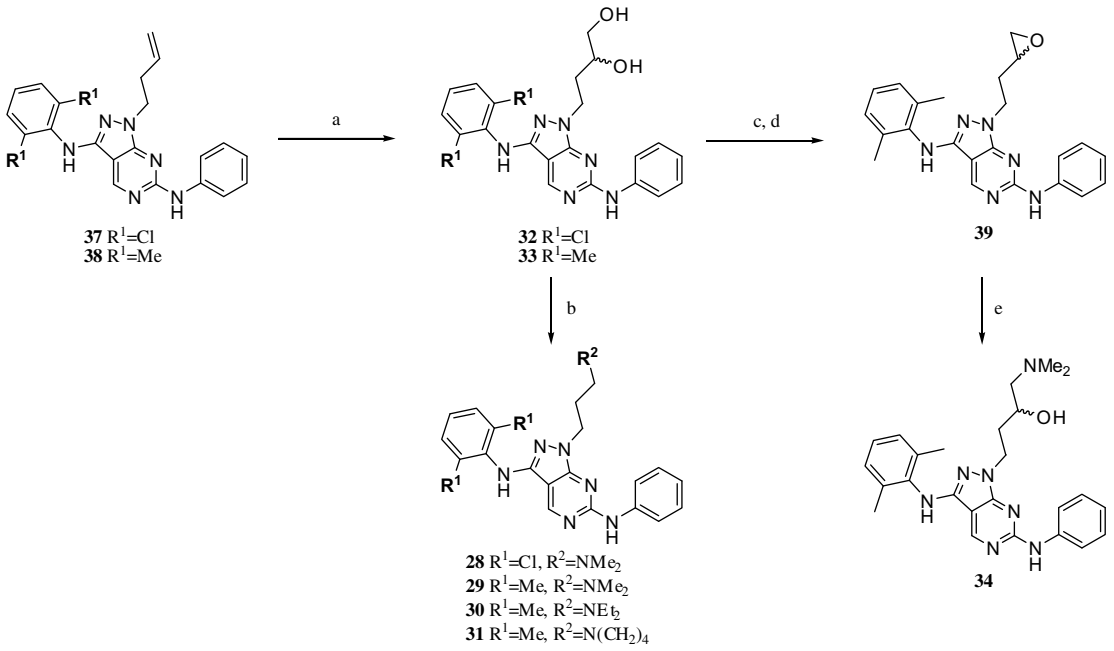

Scheme 4. Reagents and conditions: (a) OsO_4, NMO, acetone/H_2O, 87%; (b) i—$NaIO_4$, acetone/H_2O, ii—$\mathbf{R^2}$H·HCl, Et_3N, $NaBH(OAc)_3$, 1,2-dichloroethane, 51–52% (compounds **28** and **29**) or $\mathbf{R^2}$H, AcOH, $NaBH(OAc)_3$, 1,2-dichloroethane, 21–25% (compounds **30** and **31**); (c) *p*-TsCl, pyridine, CH_2Cl_2, 64%; (d) NaOMe, $CHCl_3$/MeOH, 0 °C, 88%; (e) $MeNH_2$, EtOH, 40 °C, 27%.

Table 4
Kinase selectivity for compounds **1a**, **13,** and **14** (K_i, μM).[a]

Kinase	1a	13	14
ACK1	0.020	0.003	0.003
LCK	0.013	0.00004	0.011
BTK	0.078	0.00025	0.125
KDR	>25	1.59	>12.5
Tie-2	>8.3	1.16	>2.5
Jak3	0.074	0.17	>12.5

[a] Values are means of at least two experiments.

Acknowledgments

We are grateful to our colleagues Merrill Ayres for ACK1 protein expression, and George Tonn and Monica Sweany for generating PK data.

References and notes

1. (a) Manser, E.; Leung, T.; Salihuddin, H.; Tan, L.; Lim, L. *Nature* **1993**, *363*, 364; (b) Manser, E.; Leung, T.; Salhihuddin, H.; Zhao, Z. S.; Lim, L. *Nature* **1994**, *367*, 40; (c) Manser, E.; Chong, C.; Zhao, Z. S.; Leung, T.; Michael, G.; Hall, C.; Lim, L. *J. Biol. Chem* **1995**, *270*, 25070; (d) Nur, E. K. A.; Zhang, A.; Keenan, S. M.; Wang, X. l.; Seraj, J.; Satoh, T.; Meiners, S.; Welsh, W. *J. Mol. Cancer Res.* **2005**, *3*, 297.
2. (a) Yang, W.; Lo, C. G.; Dispenza, T.; Cerione, R. A. *J. Biol. Chem.* **2001**, *276*, 17468; (b) Teo, M.; Tan, L.; Lim, L.; Manser, E. *J. Biol. Chem.* **2001**, *276*, 18392.
3. van der Horst, E. H.; Degenhardt, Y. Y.; Strelow, A.; Slavin, A.; Chinn, L.; Orf, J.; Rong, M.; Li, S.; See, L.-H.; Nguyen, K. Q. C.; Hoey, T.; Wesche, H.; Powers, S. *Proc. Natl. Acad. Sci. U.S.A.* **2005**, *102*, 15901.
4. (a) Mahajan, N. P.; Whang, Y. E.; Mohler, J. L.; Earp, H. E. *Cancer Res.* **2005**, *65*, 10514; (b) Mahajan, N. P.; Liu, Y.; Majumder, S.; Warren, M. R.; Parker, C. E.; Mohler, J. L.; Earp, H. S.; Whang, Y. E. *Proc. Natl. Acad. Sci. U.S.A.* **2007**, *104*, 8438.
5. Unpublished results.
6. The K_i assay for ACK1 has been described in detail in: Xiao, S.-H.; Farrelly, F.; Anzola, J.; Crawford, D.; Jiao, J.X; Liu J.; Ayres, M.; Li, S.; Huang, L.; Sharma R.; Kayser F.; Wesche, H.; Young, S.W. *Anal. Biochem.* **2007,** *267*, 179. Briefly, histidine(6) tagged truncated ACK1 (aa 117–489) were over expressed and purified to apparent homogeneity from SF9 cells using baculovirus expression system. A biotinylated peptide (AIRLKEEEI-YFFFFAKKK-amide) substrate is phosphorylated by ACK1 in the presence of various concentrations of ATP. The phosphorylated peptide is detected with electrochemiluminescence using phospho-tyrosine-specific mAb-labeled with ruthenium (II) tribipyridine (BV-Tag™), and streptavidin coated paramagnetic beads. K_is were generated by fitting the dose response data to the Morrison equation.
7. *ACK1 cell-based assay IC_{50} determination:* The assay relies upon the fact that ACK1 is heavily autophosphorylated in proliferating, adherent cells, and upon detachment ACK1 becomes de-phosphorylated very rapidly. When attached to plastic, ACK1 auto-phosphorylation is detectable within minutes, and reaches a maximum within 2 h. For this experiment, 293 cells stably expressing Flag-tagged ACK1 are detached from their culture dish with PBS/EDTA. After a PBS wash, cells are pre-incubated in suspension with DMSO or compound. Next, the samples are either lysed directly (control) or allowed to re-attach in medium containing 10% FCS on tissue culture dishes for 2 h prior to lysis. The inhibition of ACK1 auto-phosphorylation is determined by anti p-Tyr WB after Flag IP.
8. (a) Snow, R. J.; Cardozo, M. G.; Morwick, T. M.; Busacca, C. A.; Dong, Y.; Eckner, R. J.; Jacober, S.; Jakes, S.; Kapadia, S.; Lukas, S.; Panzenbeck, M.; Peet, G. W.; Peterson, J. D.; Prokopowicz, A. S.; Sellati, R.; Tolbert, R. M.; Tschantz, M. A.; Moss, N. *J. Med. Chem.* **2002**, *45*, 3394; (b) Goldberg, D. R.; Butz, T.; Cardozo, M. G.; Eckner, R. J.; Hammach, A.; Huang, J.; Jakes, S.; Kapadia, S.; Kashem, M.; Lukas, S.; Morwick, T. M.; Penzenbeck, M.; Patel, U.; Pav, S.; Peet, G. W.; Peterson, J. D.; Prokopowicz, A. S.; Snow, R. J.; Sellati, R.; Takahashi, H.; Tan, J.; Tschantz, M. A.; Wang, X.-J.; Wang, Y.; Wolak, J.; Xiong, P.; Moss, N. *J. Med. Chem.* **2003**, *46*, 1337.
9. All new compounds described herein were characterized by mass spectroscopy and ^{1}H NMR, and were determined to be of >95% purity by reverse-phase HPLC.
10. Monosubstituted hydrazines were synthesized by reacting hydrazine hydrate with the appropriate alkyl halide in refluxing ethanol overnight followed by distillation.
11. For a discussion of the relationship between physical properties with successful drug development, see e.g.: Lipinski, C. A. *J. Pharmacol. Toxicol. Methods* **2000**, *44*, 235.